Expected Number of Fixed Points in Boolean Networks with Arbitrary Topology

Fumito Mori[1,*] and Atsushi Mochizuki[1,2]
[1]Theoretical Biology Laboratory, RIKEN, Wako 351-0198, Japan
[2]CREST, JST 4-1-8 Honcho, Kawaguchi 332-0012, Japan

(Received 28 April 2017; published 14 July 2017)

Boolean network models describe genetic, neural, and social dynamics in complex networks, where the dynamics depend generally on network topology. Fixed points in a genetic regulatory network are typically considered to correspond to cell types in an organism. We prove that the expected number of fixed points in a Boolean network, with Boolean functions drawn from probability distributions that are not required to be uniform or identical, is one, and is independent of network topology if only a feedback arc set satisfies a stochastic neutrality condition. We also demonstrate that the expected number is increased by the predominance of positive feedback in a cycle.

DOI: 10.1103/PhysRevLett.119.028301

Optimizing network topology is a feasible strategy to improve the functional characteristics of network systems [1–4]. Therefore, the relationships between topological properties and the dynamical characteristics of these systems have attracted a considerable amount of research interest, and challenges to obtaining their analytical descriptions have been addressed. Boolean networks (BNs) [5–8], which serve as models for complex networks in biological [9–11], technological [12,13], and sociological systems [14,15], even today still have the potential to provide novel analytical methods to connect dynamics with static network structures due to their simplicity. While chaos-order transitions have been investigated in randomly constructed BNs (RBNs) [16–19], recent studies have revealed the effects of network topologies on the stability of their dynamics [20,21]. Once it was proved that the average number of attractors in an RBN grows faster than any power law with network size [22], the scaling behaviors of the number and size of attractors for BNs with different topologies and distributions of Boolean functions were determined [23–26]. In this manner, interest in BNs with special topologies, including small-world [27] and scale-free [28–30] networks, has increased.

A fundamental characteristic of a BN is the number of fixed points (FPs). A plurality of FPs is required for cell diversity because an FP can be assumed to represent a gene expression pattern that determines cell identity in cell differentiation [31–34]. It has been pointed out that the average number of FPs in an RBN is only one and, thus, real gene regulatory systems should have special structures [35]. These may be nonrandom network topologies or nonrandom regulatory functions, and can generate a sufficient number of FPs.

A case-by-case analysis is indispensable to approaching this issue because Boolean dynamics depend on both network topology and the assignment of Boolean functions. As an extreme case, the upper bound of the number of FPs in a BN under the restriction of a (signed) network topology has been described in terms of the minimum (positive) feedback vertex set [36,37]. This directly provides the necessary condition for a plurality of FPs in (positive) cycle structures [38,39].

However, the upper bound does not tell us a typical number of FPs. The expected number of FPs under the topological restriction should be obtained, because in many real cases, it is difficult to determine regulation functions whereas network topology can be observed. Once the expected number is formulated in terms of network topologies, it is clarified whether an increase in the number of cycles in a BN is relevant to increasing the expected number of FPs along with the upper bound. Moreover, it is determined whether positive cycles in a signed BN [37] effectively contribute to increasing the expected number.

As well as network topology, the presence of biases in Boolean functions will be important for the expected number. Although the expected number under no bias has been easily calculated and it is independent of network topology [40], biases should not be neglected because they have been observed in real systems [41]. It is known that biases in favor of either high or low frequency in on-state outputs (called p bias) [16,17] and high frequency of canalizing inputs [18,41–43] cause chaos-order transitions in an RBN. Therefore, their influence on the expected number should also be clarified.

We consider a BN described as

$$x_i(t+1) = f_i[\{x_j(t); j \in \boldsymbol{J}_i\}], \tag{1}$$

where x_i and f_i are a Boolean variable and a Boolean function of the vertex i, respectively. All subscripts in this Letter are indices of vertices $i = 1, \ldots, N$, where N denotes the total number of vertices. The variable x_i, which takes $x_i = 0$ for the off state and $x_i = 1$ for the on state at every discrete time instant, is updated by f_i. In a BN with the synchronous update scheme, all variables are updated at the same time. To simulate more realistic situations, the asynchronous update scheme is also often employed [44,45]. Since FPs do not depend on the choice of update scheme, we can employ either scheme. A set of input vertices to vertex i is denoted as $\boldsymbol{J_i}$. Thus, f_i is a function of $\{x_j; j \in \boldsymbol{J_i}\}$.

A link from vertex j to i represents one of the following three conditions: (i) f_i takes the input variable x_j. (ii) In addition to condition (i), f_i is dependent on x_j; i.e.,

$$f_i(x_j = 0, \{x_k; k \in \boldsymbol{J_i} - j\}) \neq f_i(x_j = 1, \{x_k; k \in \boldsymbol{J_i} - j\}) \tag{2}$$

holds for at least one state of $\{x_k; k \in \boldsymbol{J_i} - j\}$. (iii) In addition to conditions (i) and (ii), f_i is monotonically dependent on x_j; i.e., only either

$$f_i(x_j = 0, \{x_k; k \in \boldsymbol{J_i} - j\}) \leq f_i(x_j = 1, \{x_k; k \in \boldsymbol{J_i} - j\}) \tag{3}$$

or

$$f_i(x_j = 0, \{x_k; k \in \boldsymbol{J_i} - j\}) \geq f_i(x_j = 1, \{x_k; k \in \boldsymbol{J_i} - j\}) \tag{4}$$

holds for any state of $\{x_k; k \in \boldsymbol{J_i} - j\}$. Equation (3) [Eq. (4)] corresponds to a monotonically increasing [decreasing] function of x_j. Simultaneously, link $j \to i$ represents activation (inhibition) interaction, and can be called a positive (negative) link [37]. Any link condition can be employed for our theory.

We assume that while network topology (directed links and vertices) is fixed, f_i is drawn from a probability distribution of Boolean functions denoted by $P_i(f_i)$ (Fig. 1). The links defined by any one of conditions (i), (ii), and (iii) restrict possible functions, i.e., $P_i(f_i) = 0$ if f_i contradicts the link condition. The normalization condition is described as $\sum_{f_i} P_i(f_i) = 1$, where the summation is over all possible functions of f_i. We see an example shown in Figs. 2(a) and 2(b): vertex i has three input vertices. If link condition (iii) is employed, since each of functions I and J is a nonmonotonic function of x_1 and x_2, $P_i(f_i = I, J) = 0$ is assumed. Since network topology designates only $P_i(f_i) = 0$, further arrangements, such as $P_i(f_i = A)$ and $P_i(f_i = B)$, are needed.

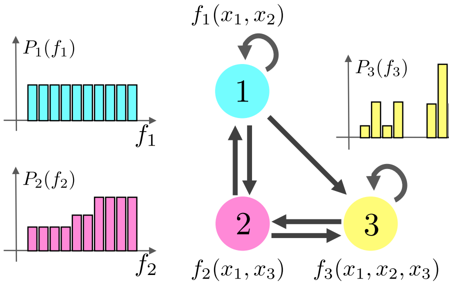

FIG. 1. An example set of a Boolean network and probability distributions of Boolean functions. Boolean function f_i, assigned to vertex i, is drawn from its probability distribution $P_i(f_i)$. Under link condition (i), a graph of $P_i(f_i)$ can have $2^{2^{K_i}}$ (the total number of Boolean functions) bars at most, where K_i is the number of input links to vertex i. Under link condition (ii) or (iii), a graph has less than $2^{2^{K_i}}$ bars. In this example, uniform, biased, and more complicated distributions are illustrated for $P_1(f_1)$, $P_2(f_2)$, and $P_3(f_3)$.

Let us present some typical distributions of $P_i(f_i)$. In the case of p bias [16,17], f_i is randomly generated and the on state is allocated as its output value for a certain input state with probability p. When either link condition (ii) or (iii) is employed, the contradictory functions are discarded. Thus, the p-biased Boolean functions tend to output on state when $p > 0.5$. To explain the canalizing bias [18,41–43], we revisit the example in Fig. 2. Function A is called a canalizing function of x_1 because if the input variable x_1 is fixed to either 0 or 1 ($x_1 = 1$ in this case), its output state is uniquely determined independently of x_2 and x_3. Hence, x_1 is called a canalizing input of function A. In this manner, a K-variable Boolean function takes 0 to K canalizing inputs. Under the canalizing bias, percentages of canalizing inputs are controlled, where some additional rules are required to set up $P_i(f_i)$. The canalizing bias has been observed in real transcriptional systems [41]. More general distributions can also be considered in our theory.

At an FP, state $x_i(t)$ prior to update and its output state $x_i(t+1)$ are equal for any i. Thus, when both a directed network and a set of Boolean functions $\{f_i; i = 1, \ldots, N\}$ are given, the number of FPs is uniquely determined as

$$n(\{f_i\}) = \sum_{x_1=0,1} \cdots \sum_{x_N=0,1} \prod_{i=1}^{N} \delta[x_i, f_i(\{x_j; j \in \boldsymbol{J_i}\})], \tag{5}$$

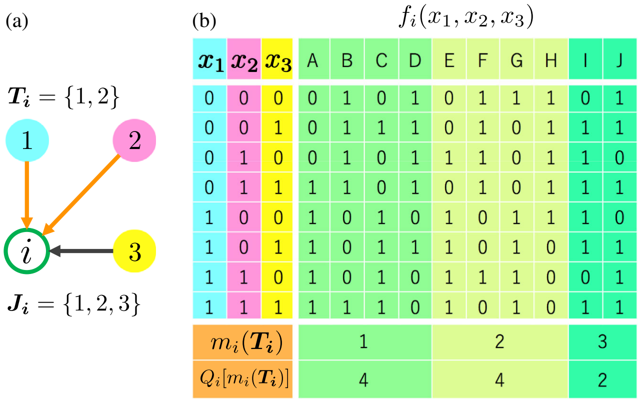

			$f_i(x_1, x_2, x_3)$									
$\boldsymbol{x_1}$	$\boldsymbol{x_2}$	$\boldsymbol{x_3}$	A	B	C	D	E	F	G	H	I	J
0	0	0	0	1	0	1	0	1	1	1	0	1
0	0	1	0	1	1	1	0	1	0	1	1	1
0	1	0	0	1	0	1	1	1	0	1	1	0
0	1	1	1	1	0	1	0	1	0	1	1	1
1	0	0	1	0	1	0	1	0	1	1	1	0
1	0	1	1	0	1	1	1	0	1	0	1	1
1	1	0	1	0	1	0	1	1	1	0	0	1
1	1	1	1	1	1	0	1	0	1	0	1	1
$m_i(\boldsymbol{T_i})$			1				2				3	
$Q_i[m_i(\boldsymbol{T_i})]$			4				4				2	

FIG. 2. (a) Schematic of a set of input vertices to vertex i, denoted by $\boldsymbol{J_i} = \{1, 2, 3\}$. Subset $\boldsymbol{T_i} = \{1, 2\}$ is employed to classify Boolean functions f_i. (b) Truth table of three-variable Boolean functions. Based on the definition of an N-equivalent class with respect to $\boldsymbol{T_i} = \{1, 2\}$, functions A–D, E–H, and I–J are organized into classes labeled as $m_i(\boldsymbol{T_i}) = 1$, 2, and 3. The number of functions in the $m_i(\boldsymbol{T_i})$th class, $Q_i[m_i(\boldsymbol{T_i})]$, depends on $m_i(\boldsymbol{T_i})$.

where $\delta[a,b]$ is the Kronecker delta: $\delta[a,b]=1$ for $a=b$ and $\delta[a,b]=0$ for $a\neq b$. Note that a and b can depend on variables $\{x_i\}$ throughout our analysis.

When Boolean functions are randomly assigned to every vertex under the restriction of a network topology, the expected number of FPs is defined by

$$\langle n\rangle = \sum_{f_1}\cdots\sum_{f_N} n(\{f_i\})\prod_{i=1}^{N} P_i(f_i). \tag{6}$$

The expected number will depend on both network topology and the probability distributions of the Boolean functions in general.

By way of preparation for the analysis, we introduce a classification method of Boolean functions called the negation- (N-)equivalent class [12]. We denote the negation of x by $\bar{x}$, and consider function $f(\{x_j; j\in \boldsymbol{J}\})$. If another function g is given by $g(\{x_j; j\in \boldsymbol{J}\})\equiv f(\{\bar{x}_j; j\in \boldsymbol{U}\},\{x_{j'}; j'\in \boldsymbol{J}-\boldsymbol{U}\})$, where $\boldsymbol{U}$ is an arbitrary subset of $\boldsymbol{J}$, f, and g are N equivalent. An N-equivalent class is defined as a set of all functions that are N equivalent to one another. We tighten the definition, and further divide the class as follows (Fig. 2): $\boldsymbol{T}$ is a given subset of $\boldsymbol{J}$. If g is given by $g(\{x_j; j\in \boldsymbol{J}\})\equiv f(\{\bar{x}_j; j\in \boldsymbol{U}\},\{x_{j'}; j'\in \boldsymbol{T}-\boldsymbol{U}\},\{x_k; k\in \boldsymbol{J}-\boldsymbol{T}\})$, where $\boldsymbol{U}$ is an arbitrary subset of $\boldsymbol{T}$, f and g are N equivalent with respect to $\boldsymbol{T}$. An N-equivalent class with respect to $\boldsymbol{T}$ is defined as a set of all functions that are N equivalent to one another with respect to $\boldsymbol{T}$. The integer index $m(\boldsymbol{T})$ is employed to represent the $m(\boldsymbol{T})$th N-equivalent class with respect to $\boldsymbol{T}$. We denote the set and the number of functions in the $m(\boldsymbol{T})$th N-equivalent class by $\boldsymbol{F}[m(\boldsymbol{T})]$ and

$$Q[m(\boldsymbol{T})]\equiv \sum_{f\in \boldsymbol{F}[m(\boldsymbol{T})]} 1, \tag{7}$$

respectively. When the N-equivalent class for f_i is discussed, we use the notations $\boldsymbol{J_i}$, $\boldsymbol{T_i}$, $m_i(\boldsymbol{T_i})$, $\boldsymbol{F_i}[m_i(\boldsymbol{T_i})]$, and $Q_i[m_i(\boldsymbol{T_i})]$. All $f_i\in \boldsymbol{F_i}[m_i(\boldsymbol{T_i})]$ satisfy the same link conditions.

An example of this classification is shown in Fig. 2. Function A has only activation links while functions B,C, and D have one or two inhibition links. Thus, in N-equivalent functions with respect to $\boldsymbol{T_i}$, only the roles of the links $j(\in \boldsymbol{T_i})\to i$ are different.

We define the concept of *stochastic neutrality* to characterize a directed link as follows: link $j\to i$ is stochastically neutral if $P_i(f_i)=P_i(g_i)$ holds for any pair of $f_i(x_j,\{x_k; k\in \boldsymbol{J_i}-j\})$ and $g_i(x_j,\{x_k; k\in \boldsymbol{J_i}-j\})\equiv f_i(\bar{x}_j,\{x_k; k\in \boldsymbol{J_i}-j\})$. Remember that g_i is the N-equivalent function of f_i with respect to j. Thus, when $\boldsymbol{T_i}$ is a given subset of $\boldsymbol{J_i}$ and all links from vertices $j\in \boldsymbol{T_i}$ to vertex i are stochastically neutral, $P_i(f_i)$ can be written as

$$P_i\Big[f_i\in \boldsymbol{F_i}[m_i(\boldsymbol{T_i})]\Big] = \tilde{P}_i[m_i(\boldsymbol{T_i})], \tag{8}$$

where $\tilde{P}_i[m_i(\boldsymbol{T_i})]$ is a function that only depends on $m_i(\boldsymbol{T_i})$ instead of f_i. This distribution must satisfy the normalization condition described as

$$\sum_{m_i(\boldsymbol{T}_i)=1,2,\cdots}\;\sum_{f_i\in \boldsymbol{F_i}[m_i(\boldsymbol{T_i})]} P_i(f_i) = \sum_{m_i(\boldsymbol{T}_i)=1,2,\cdots} \tilde{P}_i[m_i(\boldsymbol{T_i})]Q_i[m_i(\boldsymbol{T_i})] = 1. \tag{9}$$

When link $j\to i$ is stochastically neutral, the probability that the link is activation interaction is equal to the probability that it is inhibition interaction; the probabilities that non-monotonic functions are assigned can be nonzero under link condition (i) or (ii).

We emphasize that all links are stochastically neutral when the Boolean functions are randomly generated under the p bias or the canalizing bias because all f_i in $\boldsymbol{F_i}[m_i(\boldsymbol{J_i})]$ have the same number of on-state outputs and the same canalizing inputs; consequently, $P_i[f_i\in \boldsymbol{F_i}[m_i(\boldsymbol{J_i})]] = \tilde{P}_i[m_i(\boldsymbol{J_i})]$. In this sense, stochastic neutrality is commonly realized.

Our theorem below is described in terms of the feedback arc set (FAS) [46]. An FAS is defined as a subset of links containing at least one link of every cycle in a directed network. Therefore, the removal of the FAS renders the network acyclic (Fig. 3). In general, FAS is not unique, nor is it required to have a minimum size. For a given network, the following theorem holds:

Theorem.—If a set of stochastically neutral links is an FAS, $\langle n\rangle = 1$.

Proof.—We sort all vertices in the network as follows: the removal of the stochastically neutral links from the original network yields an acyclic network. We can apply an *acyclic ordering* to the acyclic network because every acyclic network has such an ordering of its vertices [46]. An acyclic ordering assigns integer numbers i $(1\leq i\leq N)$ to every vertex, where $j<i$ holds for every link $j\to i$. We assign the same set $\{i\}$ to the original network. Now, $j<i$ holds for every link $j\to i$ except for the stochastically neutral links in the original network.

We denote the set of vertices that are end points of the stochastically neutral links by $\boldsymbol{Z}$. For $i\in \boldsymbol{Z}$, $\boldsymbol{T_i}\subseteq \boldsymbol{J_i}$ is assumed such that links $j\in \boldsymbol{T_i}\to i$ are stochastically neutral and $j\in \boldsymbol{J_i}-\boldsymbol{T_i}\to i$ are not. For $i\in \boldsymbol{Z}$, using $\boldsymbol{T_i}$, the summation can be expressed as

$$\sum_{f_i\in \boldsymbol{F_i}[m_i(\boldsymbol{T_i})]} \delta[x_i, f_i(\{x_j; j\in \boldsymbol{J_i}\})] = R_i[m_i(\boldsymbol{T_i}), x_i, \{x_j; j\in \boldsymbol{J_i}-\boldsymbol{T_i}\}]Q_i[m_i(\boldsymbol{T_i})], \tag{10}$$

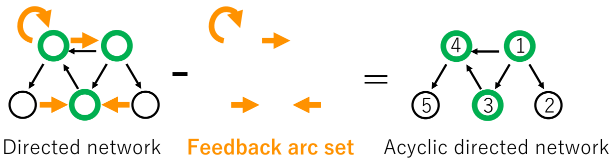

FIG. 3. Definition of feedback arc set (FAS). The bold arrows and circles in the original network correspond to links forming the FAS and vertices taking these links, respectively. Numbers 1–5 in the acyclic network represent an acyclic ordering. Therefore, $j<i$ holds for any link $j\to i$.

where $\sum_{x_i} R_i[m_i(\boldsymbol{T_i}), x_i, \{x_j; j \in \boldsymbol{J_i} - \boldsymbol{T_i}\}] = 1$ holds (see the Supplemental Material [47]). Substituting Eq. (5) into Eq. (6) and using Eqs. (8) and (10),

$$\langle n\rangle = \left(\prod_{i\in \boldsymbol{Z}} \sum_{m_i(\boldsymbol{T_i})=1,2,\cdots}\right)\left(\prod_{i\notin \boldsymbol{Z}}\sum_{f_i}\right) \left(\prod_{i\in \boldsymbol{Z}}\tilde{P}_i[m_i(\boldsymbol{T_i})]Q_i[m_i(\boldsymbol{T_i})]\right)\left(\prod_{i\notin \boldsymbol{Z}}P_i(f_i)\right) \sum_{x_1=0,1}\cdots\sum_{x_N=0,1}\left(\prod_{i\in \boldsymbol{Z}}R_i[m_i(\boldsymbol{T_i}),x_i,\{x_j;j\in \boldsymbol{J_i}-\boldsymbol{T_i}\}]\right) \left(\prod_{i\notin \boldsymbol{Z}}\delta[x_i,f_i(\{x_j;j\in \boldsymbol{J_i}\})]\right) = 1, \tag{11}$$

where the summations $\sum_{x_1}\cdots\sum_{x_N}$ can be carried out in the inverse acyclic order. □

Equation (11) indicates that a probability for $n \geq n'$ is at most $1/n'$, and will be smaller in general (see also Fig. 4). In other words, a BN does not produce a large plurality of FPs in most cases. The noteworthy finding is that both network topology and biases in favor of the on-state outputs and the canalizing inputs are irrelevant to the plurality of the FPs, though critical for chaos-order transition. The theorem further indicates that the necessary condition for changing $\langle n\rangle$ is violating stochastic neutrality on all links in at least one cycle.

We now consider a network containing ν vertex-disjoint cycles, and introduce the symmetric violation of stochastic neutrality for all links on ν cycles. We assume that links directly connecting any pair of vertices at the ηth cycle do not exist, except for the links of the ηth cycle. When link $j \to i$ is on one of the ν cycles, vertex i has

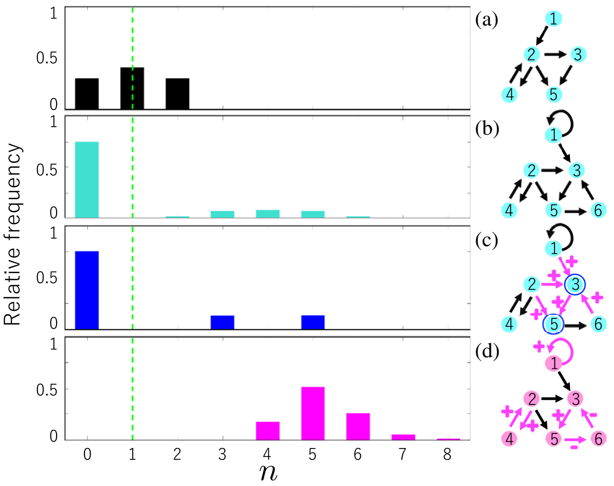

FIG. 4. Numerically obtained frequency distributions of the number of FPs for each BN (a)–(d). (a),(b) Boolean functions for all vertices were randomly generated under the p bias ($p = 0.6$). (c) The functions $f_{3,5}$ were assumed to be only AND functions. (d) The links labeled as + and − were constrained in positive and negative interactions, respectively. The average values were (a)–(c) $\langle n\rangle = 1.0$ and (d) 5.2.

$$\begin{aligned} P_i[f_i \in \boldsymbol{F}_i^{j+}[m_i(\boldsymbol{J_i})]] &= \tilde{P}_i[m_i(\boldsymbol{J_i})] + \psi_i[m_i(\boldsymbol{J_i})], \\ P_i[f_i \in \boldsymbol{F}_i^{j-}[m_i(\boldsymbol{J_i})]] &= \tilde{P}_i[m_i(\boldsymbol{J_i})] - \psi_i[m_i(\boldsymbol{J_i})], \end{aligned} \tag{12}$$

where $\boldsymbol{F}_i^{j+(-)}[m_i(\boldsymbol{J_i})] \subset \boldsymbol{F_i}[m_i(\boldsymbol{J_i})]$ is the set of monotonically increasing (decreasing) functions of x_j. If f_i is a nonmonotonic function of x_j, $P_i[f_i] = 0$. The weight parameter $\psi_i[m_i(\boldsymbol{J_i})]$ can be tuned in the range $-\tilde{P}_i[m_i(\boldsymbol{J_i})] \leq \psi_i[m_i(\boldsymbol{J_i})] \leq +\tilde{P}_i[m_i(\boldsymbol{J_i})]$. When $\psi_i[m_i(\boldsymbol{J_i})] = +(-)\tilde{P}_i[m_i(\boldsymbol{J_i})]$ for any $m_i(\boldsymbol{J_i})$, link $j \to i$ is always positive (negative). The other vertices, not on the ν cycles, have $P_i[f_i \in \boldsymbol{F_i}[m_i(\boldsymbol{J_i})]] = \tilde{P}_i[m_i(\boldsymbol{J_i})]$.

Under the above assumptions, we obtain the expected number of FPs when the symmetric violation of stochastic neutrality is introduced for all ν cycles:

$$\langle n\rangle = \prod_{\eta=1}^{\nu}\left(1 + \prod_{i=C(1,\eta)}^{C(l(\eta),\eta)}\sum_{m_i(\boldsymbol{J_i})} s_i[m_i(\boldsymbol{J_i})]\psi_i[m_i(\boldsymbol{J_i})]Q_i[m_i(\boldsymbol{J_i})]\right), \tag{13}$$

where $C(k,\eta)$ and $l(\eta)$ represent the kth vertex and the length of the ηth cycle, respectively. Coefficient $s_i[m_i(\boldsymbol{J_i})]$ is the ratio of the number of functions $f_i \in \boldsymbol{F}_i^{j+}[m_i(\boldsymbol{J_i})]$ satisfying $f_i(x_j = 0, \{x_{j'}; j' \in \boldsymbol{J_i} - j\}) < f_i(x_j = 1, \{x_{j'}; j' \in \boldsymbol{J_i} - j\})$ for state $\{x_{j'}; j' \in \boldsymbol{J_i} - j\}$ to $Q_i[m_i(\boldsymbol{J_i})]/2$. This ratio is independent of state $\{x_{j'}; j' \in \boldsymbol{J_i} - j\}$. A detailed derivation is given in the Supplemental Material [47].

In Eq. (13), the contribution of link $j \to i$ is given by $\sum_{m_i(\boldsymbol{J_i})} s_i\psi_i Q_i$, the sign of which can be easily obtained even if s_i and Q_i are unknown when only either $\psi_i[m_i(\boldsymbol{J_i})] > 0$ or $\psi_i[m_i(\boldsymbol{J_i})] < 0$ is assumed for all $m_i(\boldsymbol{J_i})$. The total contribution of the ηth cycle, the sign of which corresponds to the predominance of either positive or negative feedback on the ηth cycle, changes $\langle n\rangle$. Although positive and negative feedbacks are known as the necessary conditions for the existence of multiple FPs and a limit-cycle oscillation, respectively [37–39], the sufficiency of changing $\langle n\rangle$ is verified. Equation (13) also provides the upper and lower bounds of $\langle n\rangle$, which are expressed as $0 \leq \langle n\rangle \leq 2^{\nu}$.

Finally, we numerically show the frequency distributions of n. In Fig. 4, example (a) has a different network topology from those of (b),(c), and (d). In (b),(c), and (d), different $\{P_i(f_i)\}$ were assumed. We employed link condition (ii) and generated f_i randomly under p bias ($p = 0.6$). In (a) and (b), $P_i(f_i) \propto p^M(1-p)^{2^{K_i}-M}$ if f_i had M on-state outputs. Examples (c) and (d) contained further assumptions. In (c), P_i for $i = 3, 5$ were replaced by $P_3(f_3 = x_1x_2x_6) = P_5(f_5 = x_2x_3) = 1$. In (d), the above-mentioned symmetric violation of stochastic neutrality was introduced into three cycles, where $\psi_i[m_i(\boldsymbol{J_i})] = \pm\tilde{P}_i[m_i(\boldsymbol{J_i})]$ were assumed consistent with the signs shown. We generated 10^5 realizations of $\{f_i\}$ for each network.

The relative frequency distributions of examples (a)–(d) are shown in Fig. 4. In (b) and (c), relative frequency for $n = 0$ was approximately 75%, whereas $n \geq 6$ was rarely observed. Because of the theorem, the average was 1 in (a)–(c). In (d), $\langle n \rangle = 5.2$ was obtained, since three positive and no negative feedbacks were realized.

Controlling only network topology does not contribute to changing $\langle n \rangle$ even under a p bias and a canalizing bias. The sufficient condition for increasing $\langle n \rangle$ is the predominance of positive feedbacks. Real systems exhibiting a large plurality of FPs would not only have many topological cycles, but would also contain elaborate regulatory rules that collectively compose positive feedbacks.

The expected number of periodic attractors is also important, since there is an alternative idea whereby a periodic attractor can correspond to a cell type in cell differentiation [48]. A key in our formulation for FPs is the invariance of variable R_i under $x_j \to \bar{x}_j$ ($j \in \boldsymbol{T_i}$ and $j \neq i$). In a similar way, creating a new invariant variable by introducing an appropriate class of functions can provide a key technique to analyze the expected number of attractors with a certain oscillation period in a BN with arbitrary topology.

We thank Masashi Tachikawa and Takashi Okada for valuable comments. This work was supported by the "Creation of Fundamental Technologies for Understanding and Control of Biosystem Dynamics (JPMJCR13W6)," a CREST grant from the Japan Science and Technology Agency (JST), and by the iTHEMS program/iTHES project of RIKEN.

---

*fumito.mori@riken.jp

[1] T. Gross and B. Blasius, J. R. Soc. Interface **5**, 259 (2008).
[2] P. Holme and J. Saramäki, Phys. Rep. **519**, 97 (2012).
[3] F. A. Rodrigues, T. K. D. Peron, P. Ji, and J. Kurths, Phys. Rep. **610**, 1 (2016).
[4] Y.-Y. Liu and A.-L. Barabási, Rev. Mod. Phys. **88**, 035006 (2016).
[5] S. A. Kauffman, J. Theor. Biol. **22**, 437 (1969).
[6] S. A. Kauffman, *Investigations* (Oxford University Press, New York, 2000).
[7] M. Aldana, S. Coppersmith, and L. P. Kadanoff, in *Perspectives and Problems in Nolinear Science* (Springer, New York, 2003), p. 23.
[8] R. Albert and A.-L. Barabási, Phys. Rev. Lett. **84**, 5660 (2000).
[9] R. Robeva and T. Hodge, *Mathematical Concepts and Methods in Modern Biology: Using Modern Discrete Models* (Academic Press, New York, 2013).
[10] M. Maucher, B. Kracher, M. Kühl, and H. A. Kestler, Bioinformatics **27**, 1529 (2011).
[11] D. P. Rosin, D. Rontani, D. J. Gauthier, and E. Schöll, Phys. Rev. Lett. **110**, 104102 (2013).
[12] T. Sasao, *Switching Theory for Logic Synthesis* (Springer Science & Business Media, New York, 2012).
[13] D. P. Rosin, *Dynamics of Complex Autonomous Boolean Networks* (Springer, New York, 2014).
[14] C. Castellano, S. Fortunato, and V. Loreto, Rev. Mod. Phys. **81**, 591 (2009).
[15] H. Sayama, I. Pestov, J. Schmidt, B. J. Bush, C. Wong, J. Yamanoi, and T. Gross, Comput. Math. Appl. **65**, 1645 (2013).
[16] B. Derrida and Y. Pomeau, Europhys. Lett. **1**, 45 (1986).
[17] B. Derrida and D. Stauffer, Europhys. Lett. **2**, 739 (1986).
[18] C. Seshadhri, Y. Vorobeychik, J. R. Mayo, R. C. Armstrong, and J. R. Ruthruff, Phys. Rev. Lett. **107**, 108701 (2011).
[19] C. Seshadhri, A. M. Smith, Y. Vorobeychik, J. R. Mayo, and R. C. Armstrong, Phys. Rev. E **94**, 012301 (2016).
[20] A. Pomerance, E. Ott, M. Girvan, and W. Losert, Proc. Natl. Acad. Sci. U.S.A. **106**, 8209 (2009).
[21] S. Squires, A. Pomerance, M. Girvan, and E. Ott, Phys. Rev. E **90**, 022814 (2014).
[22] B. Samuelsson and C. Troein, Phys. Rev. Lett. **90**, 098701 (2003).
[23] B. Drossel, T. Mihaljev, and F. Greil, Phys. Rev. Lett. **94**, 088701 (2005).
[24] B. Drossel, Phys. Rev. E **72**, 016110 (2005).
[25] V. Kaufman, T. Mihaljev, and B. Drossel, Phys. Rev. E **72**, 046124 (2005).
[26] B. Drossel, in *Reviews of Nonlinear Dynamics and Complexity* edited by, H. G. Schuster (Wiley, Weinheim, 2008), Vol. 1.
[27] C. H. A. Ferraz and H. J. Herrmann, Physica (Amsterdam) **373A**, 770 (2007).
[28] M. Aldana, Physica (Amsterdam) **185D**, 45 (2003).
[29] R. Serra, M. Villani, and L. Agostini, Physica (Amsterdam) **339A**, 665 (2004).
[30] K. Iguchi, S.-i. Kinoshita, and H. S. Yamada, J. Theor. Biol. **247**, 138 (2007).
[31] S. Huang, J. Mol. Med. (Berlin) **77**, 469 (1999).
[32] R. Thomas and M. Kaufman, Chaos **11**, 170 (2001).
[33] R. Thomas and M. Kaufman, Chaos **11**, 180 (2001).
[34] K. S. Imai, M. Levine, N. Satoh, and Y. Satou, Science **312**, 1183 (2006).
[35] A. Mochizuki, J. Theor. Biol. **236**, 291 (2005).
[36] T. Akutsu, S. Kuhara, O. Maruyama, and S. Miyano, Genome Inf. Ser. **9**, 151 (1998).
[37] J. Aracena, Bull. Math. Biol. **70**, 1398 (2008).
[38] M.-H. Shih and J.-L. Dong, Adv. Appl. Math. **34**, 30 (2005).
[39] É. Remy, P. Ruet, and D. Thieffry, Adv. Appl. Math. **41**, 335 (2008).
[40] P. M. de Espanés, A. Osses, and I. Rapaport, BioSystems **150**, 167 (2016).
[41] S. E. Harris, B. K. Sawhill, A. Wuensche, and S. Kauffman, Complexity **7**, 23 (2002).
[42] S. Squires, E. Ott, and M. Girvan, Phys. Rev. Lett. **109**, 085701 (2012).
[43] A. A. Moreira and L. A. N. Amaral, Phys. Rev. Lett. **94**, 218702 (2005).
[44] F. Greil and B. Drossel, Phys. Rev. Lett. **95**, 048701 (2005).
[45] K. Klemm and S. Bornholdt, Phys. Rev. E **72**, 055101 (2005).
[46] J. Bang-Jensen and G. Z. Gutin, *Digraphs: Theory, Algorithms and Applications* (Springer Science & Business Media, New York, 2008).
[47] See Supplemental Material at http://link.aps.org/supplemental/10.1103/PhysRevLett.119.028301 for various details of the calculations.
[48] S. Huang, G. Eichler, Y. Bar-Yam, and D. E. Ingber, Phys. Rev. Lett. **94**, 128701 (2005).